Unprecedented Halide Ion Binding by Nanoscaled Anionic Metal-Oxide Clusters

Shan She,[a,b] Mu Li,[a] Qi Li,[b] Zehuan Huang,[b] Yongge Wei*[b] and Panchao Yin*[a]

[a] Dr. S. She, M. Li, Prof P. Yin
South China Advanced Institute for Soft Matter Science and Technology & State Key Laboratory of Luminescent Materials and Devices, South China University of Technology,
Guangzhou, 510640, PR China
E-mail: yinpc@scut.edu.cn; yinpanchao@tsinghua.org.cn

[b] Dr. S. She, Q. Li, Dr. Z. Hunag, Prof. Y.G. Wei
Department of Chemistry
Tsinghua University
Beijing, 100084, PR China
E-mail: yonggewei@mail.tsinghua.edu.cn

Abstract: One halide ion (X^-) can bind on the surface of nano-scaled metal oxide clusters and form stable complex in solutions with binding constant K as 1.53×10^3. Suggested from single crystal structural analysis, multiple hydrogen bonding through the interactions between X^- and three hydroxy groups on the uncapped side of the cluster is responsible for such binding behaviors. Thanks to the availability of such supramolecular interaction in cluster systems, their catalytic activities, evaluated from the oxidation of alcohols to aldehydes, can be switched upon the introduction of halide ions and water molecules. The halide ions work as inhibitor by blocking the active sites of the clusters while they can be re-activated by the adding of water.

Introduction

The living organisms' quick adaption to surrounding environment highly relies on their controllable metabolism systems.[1] At microscale, it requires the accurate tuning of the hierarchical structures and the resulted catalytic activities of a series of enzymes in the metabolism cycles in response to external environmental changes.[2] Specifically, the enzyme performances are dominantly regulated by the enrichments of inhibitor or activator molecules for their effectiveness and the availability of multiple working states.[2c, 2d] On the other hand, as the most popular artificial catalysts, nano-materials are active towards broad types of chemical reactions and conjecture promising industry-scale applications[3]; however, the report on the 'smart' nano-catalysts that can respond to external stimulus is still at its early stage[4]. Especially, as the mimicry case of enzyme, the tuning protocol of nano-catalysts' performance through specific molecular binding is less explored.[5]

As a group of well-defined metal oxide molecular clusters with sizes ranging from 1 to 10 nm, polyoxometalates (POMs) are compatible with different solvent media, facilitating the molecular binding studies.[6] Owing to their stable, mono-dispersed structures and high solubility in various solvents, their static/dynamic structures in both crystalline and solution states can be well characterized.[6-7] Due to the change of POMs' surface densities, the possible molecular binding to POMs are expected to alter the solution behaviours of POMs.[6d, 8] On the other hand, the study on the molecular binding on POMs is also critical to extend the functionalities of metal oxide materials.[9] As one group of the most widely used cluster catalysts, the possible molecular binding on POMs is expected to stabilize their surface ligands and alter their charge densities, and thus, regulate the interaction between catalysts and substrates, finally contributing to the tuning of POMs' catalytic activities. Moreover, metal oxides are popular electrode materials for the detection of ions, gas molecules, and biomolecules resulted from their excellent redox properties.[10] Their applications in sensor can be enriched by the studies on molecular binding on POMs. Herein, the halide ion binding on 1-nm Anderson-type POMs ([(n-$C_4H_9)_4N]_3\{AlMo_6O_{18}(OH)_3[(OCH_2)_3CH_3]\}$, simplified as $AlMo_6CH_3$, has been, for the first time, designed and confirmed *via* structural studies in both crystalline and solution states. The binding dynamics has been uncovered by NMR and thermal analysis. Suggested from structural analysis, the binding behaviour can be used to block the catalytically active sites of POMs. Further monitoring of catalytic oxidation reactions has been carried out and it is confirmed that the regulating of catalytic activities of metal oxide clusters can be achieved *via* supramolecular binding of halide ions.

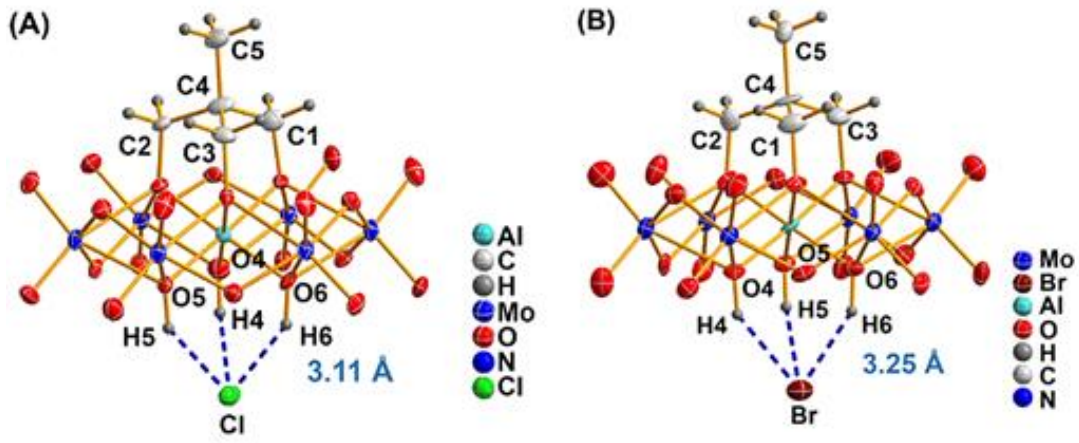

Figure 1. Molecular structures of a) $AlMo_6CH_3{\cdot}Cl$ b) $AlMo_6CH_3{\cdot}Br$, with thermal ellipsoids are drawn at the 50% probability level.

Results and Discussion

The organic functionalization of Anderson-type POMs is vital in improving POMs' stability and solubility in various solvents, facilitating the direct probing of POMs' structures in solutions.[11]

Specifically, single-side capped Anderson-type POM, is a ca. 1 nm, plate-shape molecular cluster with one side covalently functionalized by organic triol ligands (Figure 1).[11b-d] The uncapped side of POM is fully occupied by oxo and hydroxy ligands, serving as analogues to the surface of metal oxide/hydroxide nanoparticles (MOHO NPs) and bulk substrates.[11b-d]

Suggested from structural analysis, halide ions can bind onto the uncapped side of $AlMo_6CH_3$ via multiple hydrogen bonding. The single crystals of halide ion/POM complex ($AlMo_6CH_3{\cdot}X$) can be obtained by mixing appropriate amount of halide ions (X^-, X = Cl, Br) with the solutions of $AlMo_6CH_3$ in acetonitrile. Our previous study indicates that single-side organically functionalized Anderson-type POM prefer to stack with their intact side to form dimer structures (Figure 2c, and Figure S1 in supporting information).[11b] The inter-POM multiple hydrogen bonding stabilizes the dimer structure while the adding of halide ions will block POMs' hydrogen bonding sites and disassemble the dimers (Figure 2c). In the molecular structures of $AlMo_6CH_3{\cdot}X$ (Figure 1), the three μ3-oxo ligands (O4, O5, and O6) on the intact side of Anderson-type POM are protonated, driving the formation of triple hydrogen bonding to the halide ion. Suggested by the short donor-acceptor distances (typically, O4···X < 3.30 Å) (Figure 1, and Table S1 in supporting information), these hydrogen bonds are comparatively strong, and the accumulation of multiple hydrogen bonds is critical to overcome electrostatic repulsion between anionic POMs and halide ions. Additionally, since the ionic radius of Br^- is bigger than that of Cl^-, the O4···Br^- distance (3.25 Å) is longer than that of O4-Cl^- (3.11 Å), indicating the weaker hydrogen bonding interaction of $AlMo_6CH_3$···Br^- than that of $AlMo_6CH_3$···Cl^-.

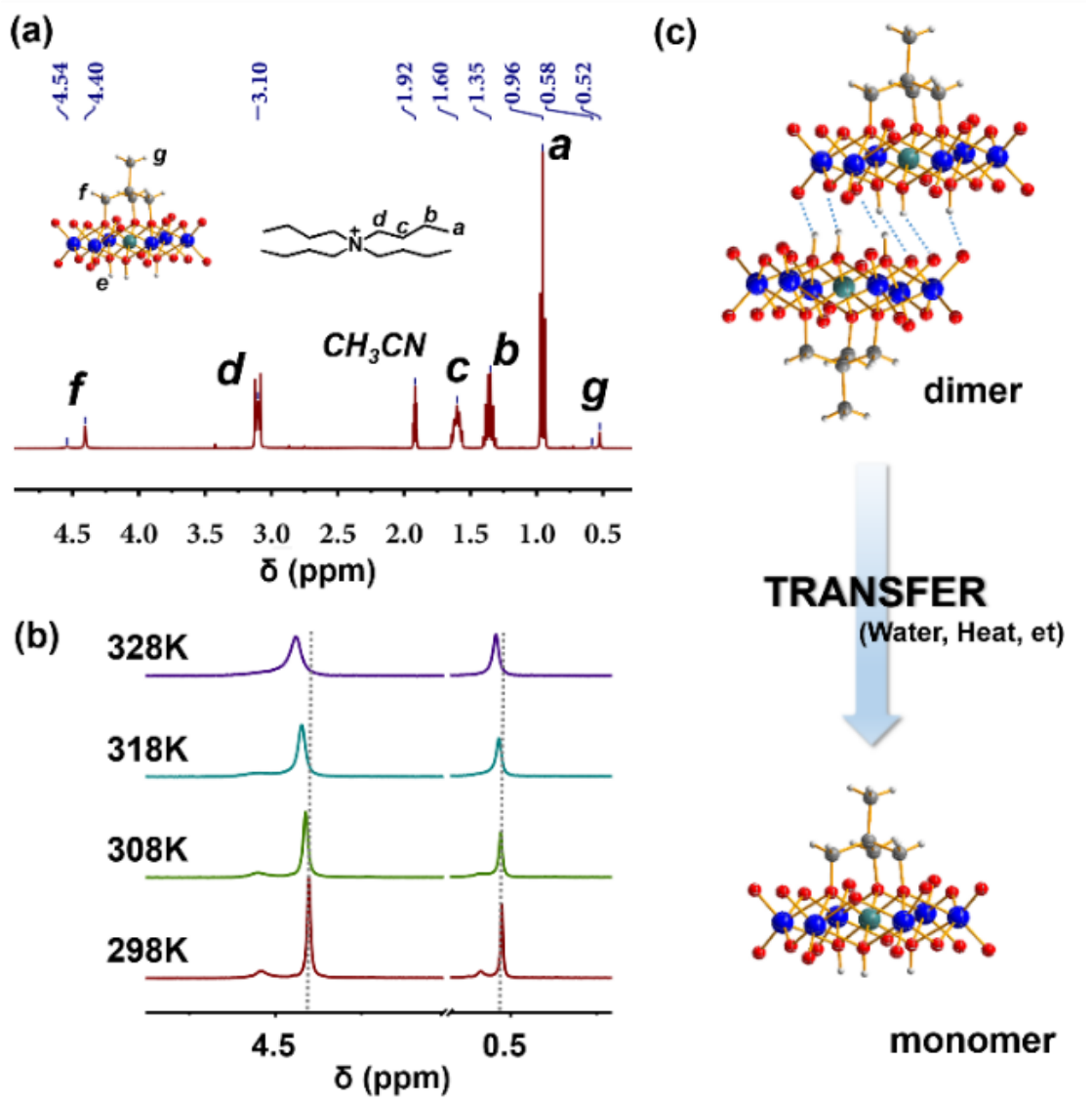

Figure 2. a) ^{1}H NMR spectrum of $AlMo_6CH_3$ at 10.0 mM in acetonitrile-d_3 at 298K; b) Variable temperature 1H NMR spectrum of $AlMo_6CH_3$ at 10.0 mM in acetonitrile-d_3; c) The transformation between dimer state and monomer state.

The halide ion binding-resulted dimer to monomer transformation of POMs in solutions has been explored by small angle X-ray scattering (SAXS) and electrospray ionized mass spectroscopy (ESI-MS). The sizes of the clusters in solutions, indexed by the radius of gyration (R_g) obtained from Guinier analysis of SAXS data, decrease from 5.1 to 4.2 Å after the adding of 6 equiv. of Cl^- to the solutions of POMs in acetonitrile (Figure S2 in supporting information), implying the disassembly of dimer to monomer POM structures.[12] In ESI-MS measurements, the binding of chloride ion and bromide ion by the POM can be clearly observed from their spectra (Figure S3 in supporting information).

This dimer/monomer transformation process in solutions can be confirmed *via* ^{1}H NMR studies. As shown in Figure 2a, two characteristic sharp resonances at 4.40 ppm and 0.52 ppm,

respectively, are assigned to the protons on the organic ligand of $AlMo_6CH_3$ anion. The integrations of the above two resonances show evidently less protons (ca. 4.8 and 2.3, respectively) than the ideal numbers of protons (6.00 and 3.00, respectively) in f and g sites, while the inconsistences can be matched coincidently by the integrations of two broad peaks (ca. 1.0 and 0.6, respectively) adjacent to the above sharp resonances, located at 4.54 ppm and 0.58 ppm, respectively. This implies that the corresponding protons exist in two different chemical environments in solutions. To further confirm that assumption, variable temperature ^{1}H NMR experiments have been conducted (Fig. 3a). With the temperature raising from 298 K to 328 K, the sharp signal at 4.40 ppm gradually downfield shifts while the resonance at 4.54 ppm is gradually broadened and almost vanishes. Finally, the integrations of the strong resonances at 328 K match with the ideal values. Moreover, when extra water is introduced to POMs' solution, it shows only a sharp resonance at 4.40 ppm in their ^{1}H NMR spectra and the integration is right 6. The co-existence of monomer/dimer leads to the different chemical environments for H_f (H_g), contributing to the division in ^{1}H NMR. The existence of monomer-dimer equilibrium in Anderson-type POM solutions can be regulated upon temperature change and the introduction of extra water by destroying the inter-POM hydrogen bonding. Similar transformation has been observed in the solutions decavanadates.[13]

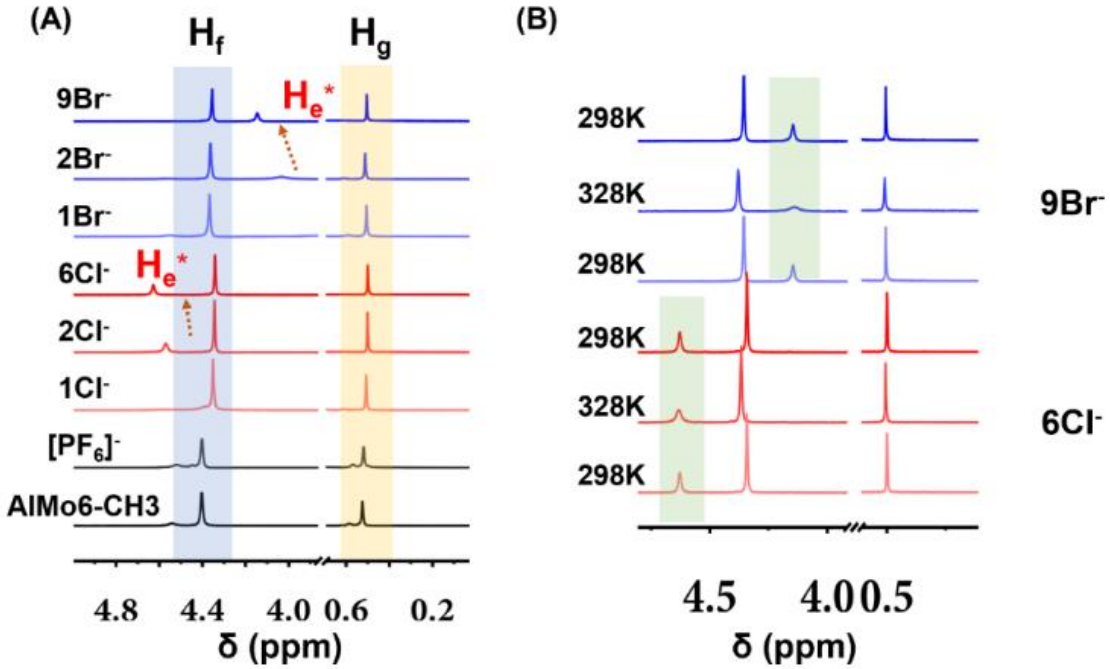

Figure 3. a) Investigation on halide ion adding into $AlMo_6CH_3$ at 10.0 mM in acetonitrile-d_3 at 298K; b) Variable temperature ^{1}H NMR spectrum to detect the hydrogen bond between POM and halide ion.

^{1}H NMR techniques can be also applied to probe the dynamic halide ion binding process by monitoring the POM-halide ion reaction solutions with various solution temperatures and molar ratios of X^-/POM. By adding one equiv. of Cl^- or Br^- into $AlMo_6CH_3$ acetonitrile solutions (10.0 mM) at 298 K, the characteristic dual resonance assigned to the dimer state disappears and turns into a single sharp one, the character for monomer POM (Figure 3a, and Figure S4 in supporting information). When the halide ion is continuously added, a new single resonance noted as H_e* appears, attributed to the three hydroxy ligands that interact with the halide ions (Figure S5 in supporting information). The resonance of H_e* shows sharp peak at 4.57 ppm when Cl^- was introduced (Cl^-/AlMo6CH3 ratio ~ 2). For the case of Br^-, it was a broad resonance at 4.03 ppm (Br^-/$AlMo_6CH_3$ ratio 2). Such differences can be attributed to the stronger interaction between $AlMo_6CH_3$ cluster and Cl^-. When the concentration of Cl^- is gradually increased to 6 equiv., the location of H_e* downfield shifts and finally settles at 4.63 ppm (Figure S6 in supporting information), indicating that such halide ion binding process is a dynamic equilibrium process. With the temperature raising from 298 K to 328 K, the signal of H_e* is gradually broadened because of the weakening of -OH···X hydrogen bond, facilitating the quick exchange of H_e at high temperatures. The process can be reversed by manipulating environmental temperature, suggesting that the hydrogen bonding-directed halide ion binding is a rapid dynamic process that highly relies on the solution temperature and halide ion concentration (Figure 3b).

As a typical technique for analysing the binding of substrates to enzymes, ITC has been applied to quantify the stability of $AlMo_6CH_3$·Cl complex data.[14] It is indicated from the data analysis of the titration experiments of Cl^- to $AlMo_6CH_3$ in acetonitrile the binding constant is 1.53×10^3 (following the formula: $K = 1/K_d(M)$) (Figure S7 in supporting information). This is comparable to the binding constant of typical hydrogen bonding to anions[15] and much higher than that of typical POM-counterion association[20], confirming that Cl^- binding to $AlMo_6CH_3$ anion can be strong to form stable complex. As typical feature for hydrogen bonding, the tri-hydroxyl hydrogen bonding donating sites on POM surface can actually bonded to various anions, including halide ions.[15] The bonding strength highly relies on charge densities and coordinating capabilities.[15] As a control experiment, the bonding affinity between PF_6^- and $AlMo_6CH_3$ ion is found to be fairly weak and no obvious association can be observed (Figure S8 in supporting information), according to ITC and ^{1}H NMR spectroscopic results. PF_6^-, a non-coordinating anion with the weakest hydrogen bonding accepting capability,[15] shows negligible hydrogen bonding interaction to POM, and thus cannot afford the anion binding event. This ensures the credibility of our characterization of Cl^-/$AlMo_6CH_3$ binding process.

The halide ion binding event can be further applied to regulate the catalytic activities of POMs by blocking their catalytic active sites. Suggested from ^{1}H-NMR monitoring results, benzyl alcohol can be oxidized to benzaldehyde under ambient condition at 60 ℃ with the existence of $AlMo_6CH_3$ as catalyst. Interestingly, the adding of appropriate amounts (6 equiv.) of Cl^- to the reaction solutions can completely stop the oxidation reactions with benzyl alcohol intact. The catalytic activities of POMs can be resumed by adding appropriate amounts (6 equiv.) of water (Figure 4, Table 1, and Discussion S2 in supporting information). Single-side capped Anderson type POMs are active catalysts for multiple types of oxidation reactions.[16] According to previous literatures, the hetero-metal ions serve as the active centres and the three hydroxy groups are the accessible sites for organic substrate molecules.[16] The binding of halide ions provides space hindrance for the accessing of organic substrates to the active sites of POMs and deactivate the catalytic functionality of POMs. The added water molecules can compete with Cl^- to bind onto the uncapped side of POMs *via* hydrogen bonding and finally resume the accessibility of active sites to substrate molecules (Figure 4). Therefore, supramolecular interactions can be used to switch the catalytic activities of POMs to off/on states by adding/getting rid of halide ions.

Figure 4. The binding of Cl^- regulated catalytic activity of POMs. Colour codes for spheres in space filling models: dark grey, H; light grey, C; red, O; cyan, Al; green, Cl; blue, Mo.

Sheme 1. The catalyzed oxidation reaction of alcohol to aldehyde by $AlMo_6CH_3$.

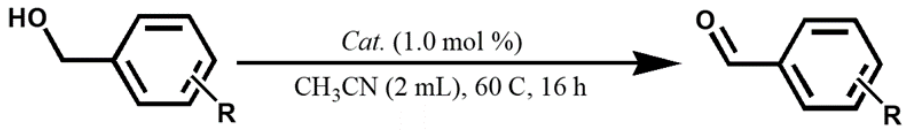

Table 1. Investigate the chloride ion influence on oxidation of benzyl alcohol with $AlMo_6CH_3$ catalysts.

Entry	Substrate	Conversion			
		$AlMo_6CH_3$	$AlMo_6CH_3{\cdot}Cl$	$AlMo_6CH_3{\cdot}6Cl$	$AlMo_6CH_3{\cdot}6Cl{\cdot}H_2O$
1	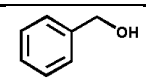	73.8 %	61.2 %	< 5 %	47.4 %
2	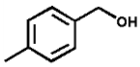	82.4 %	63.9 %	< 5 %	52.4 %
3	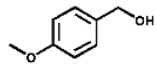	89.7 %	71.5 %	< 5 %	55.6 %
4	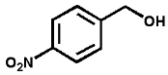	64.1 %	43.1 %	< 5 %	26.9 %
5	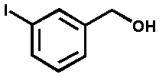	59.6 %	39.9 %	< 5 %	27.2 %

Conclusions

In conclusion, the hydrogen bonding directed halide ion binding to the surface of $AlMo_6CH_3$ has been investigated from crystalline state to solutions. The existence of multiple cooperative hydrogen bonding is critical for such binding event to overcome the electrostatic repulsion between halide ions and anionic POMs. The halide ion binding can be further used to regulate POMs' catalytic activities. This work not only enriches the supramolecular chemistry of POMs, but also provides protocols to tune the properties/functionalities of MOHO NPs *via* supramolecular interactions.

Experimental Section

General information. All chemicals were purchased and used as supplied without further purification. Acetonitrile was distilled by refluxing in the presence of CaH_2 overnight. $(NH_4)_3[AlMo_6O_{18}(OH)_6]$ was prepared according to literature[17]. The ESI-MS spectra of compounds were measured in a flow injection form, the tested concentration in hybrid was 3×10^{-4} M, the extraction cone value was 5 μL and the source temperature was 300 °C. The above tests were performed on Thermo Scientific, Q Exactive. Flash EA 1112 full-automatic microanalyses were used to analyze the elemental composition. The ^1H NMR spectra were obtained using a JOEL JNM-ECA400 apparatus.

Isothermal titration calorimetry (ITC) experiments were carried out with a TA Nano ITC apparatus in acetonitrile at 298.15 K. POM solutions was prepared by dissolving 24.6 mg $AlMo_6CH_3$ sample in 1.5 mL anhydrous acetonitrile. The solution of TBA·Cl (20 mg/mL) was used to titrate the above POM solution. The blank experiments were run by titrating TBA·Cl solution to pure anhydrous acetonitrile. The dilution effect from the blank experiments was used to calibrate the anion binding experiments. For control experiment, the solution of $TBA{\cdot}PF_6$ (20 mg/mL) was used to titrate the above POM solution. The blank experiments were run by titrating $TBA{\cdot}PF_6$ solution to pure anhydrous acetonitrile.

SAXS measurements were performed in Xeuss 2.0 system with MetalJet source installed. The POM solutions were placed in glass capillary and the detector was placed 0.5 m away from the samples.

X-ray Crystallography. Single-crystal X-ray diffraction analyses were performed on a Rigaku RAXIS-SPIDER IP diffractometer at 50 kV and 20 mA, using graphite monochromatized Mo K_α radiation (λ = 0.71073 Å) at 93.15 K. Data collection, data reduction, cell refinement, and experimental absorption correction were performed with the software package of Rigaku RAPID AUTO (Rigaku, 1998, Ver2.30). Structures were solved by direct methods and refined against F^2 by full matrix least squares. All non-hydrogen atoms, except disordered atoms, were refined anisotropically. Hydrogen atoms were generated geometrically. All calculations were performed using the SHELXS-97 program package. (CCDC:1866503, 1866504, 1873108) These data can be obtained free of charge from The Cambridge Crystallographic Data Centre via www.ccdc.cam.ac.uk/data_request/cif.

Acknowledgements

P. Yin acknowledges support from the National Natural Science Foundation of China (No.51873067), Natural Science Foundation of Guangdong Province (No. 2018A030313503) and the Fundamental Re-search Funds for the Central Universities (No. 2018JQ04). Y. Wei acknowledges support from the National Natural Science Foundation of China (No. 21471087 and 21225103). S. Shan acknowledges support from the European Commission for a Marie Curie Fellowship (PPOM-PTT, 798821).

Keywords: polyoxometalates • catalysis • clusters • anion binding • hydrogen bonding

[1] a) J. L. Wilson, *J. Chem. Edu.* **1988**, *65*, A337; b) Lehninger, L. Albert, A. L. Lehninger, Biochemistry, **1977**.

[2] a) T. Traut, Allosteric Regulatory Enzymes, **2008**; b) E. C. S. Kumar, Molecular biology and evolution, **1983**; c) D. N. Baron, Advances in enzyme regulation, **1963**; d) A. Fersht, Enzyme structure and mechanism, **1974**.

[3] a) G. Prieto, H. Tüysüz, N. Duyckaerts, J. Knossalla, G.-H. Wang, F. Schüth, *Chem. Rev.* **2016**, *116*, 14056-14119; b) Y. Zhang, X. Cui, F. Shi, Y. Deng, *Chem. Rev.* **2012**, *112*, 2467-2505.

[4] a) R. Göstl, A. Senf, S. Hecht, *Chem. Soc. Rev.* **2014**, *43*, 1982-1996; b) R. S. Stoll, S. Hecht, *Angew. Chem. Int. Ed.* **2010**, *49*, 5054-5075; c) V. Blanco, D. A. Leigh, V. Marcos, *Chem. Soc. Rev.* **2015**, *44*, 5341-5370.

[5] a) Q. Zhuang, Z. Yang, Y. I. Sobolev, W. Beker, J. Kong, B. A. Grzybowski, *ACS Cata.* **2018**, *8*, 7469-7474; b) S. Semwal, J. Choudhury, *Angew. Chem. Int. Ed.* **2017**, *56*, 5556-5560.

[6] a) M. T. Pope, A. Müller, *Angew. Chem. Int. Ed.* **1991**, *30*, 34-48; b) B. Li, W. Li, H. Li, L. Wu, *Acc. Chem. Res.* **2017**, *50*, 1391-1399; c) L. Cronin, A. Müller, *Chem. Soc. Rev.* **2012**, *41*, 7333-7334; d) P. Yin, D. Li, T. Liu, *Chem. Soc. Rev.* **2012**, *41*, 7368-7383.

[7] a) D. L. Long, E. Burkholder, L. Cronin, *Chem. Soc. Rev.* **2007**, *36*, 105-121; b) P. Yin, B. Wu, E. Mamontov, L. L. Daemen, Y. Cheng, T. Li, S. Seifert, K. Hong, P. V. Bonnesen, J. K. Keum, A. J. Ramirez-Cuesta, *J. Am. Chem. Soc.* **2016**, *138*, 2638-2643; c) P. Yin, B. Wu, T. Li, P. V. Bonnesen, K. Hong, S. Seifert, L. Porcar, C. Do, J. K. Keum, *J. Am. Chem. Soc.* **2016**, *138*, 10623-10629; d) J. M. Pigga, J. A. Teprovich, R. A. Flowers, M. R. Antonio, T. Liu, *Langmuir* **2010**, *26*, 9449-9456.

[8] J. Zhou, J. Hu, M. Li, H. Li, W. Wang, Y. Liu, R. E. Winans, T. Li, T. Liu, P. Yin, *Mater. Chem. Front.* **2018**, *2*, 2070-2075.

[9] a) B. E. Petel, W. W. Brennessel, E. M. Matson, *J. Am. Chem. Soc.* **2018**, *140*, 8424-8428; b) P. Blanchard, C. Lamonier, A. Griboval, E. Payen, *Appl. Catal. A Gen.* **2007**, *322*, 33-45.

[10] a) Y. Jimbo, N. Matsuhisa, W. Lee, P. Zalar, H. Jinno, T. Yokota, M. Sekino, T. Someya, *ACS Appl. Mater. Interf.* **2017**, *9*, 34744-34750; b) X.-C. Dong, H. Xu, X.-W. Wang, Y.-X. Huang, M. B. Chan-Park, H. Zhang, L.-H. Wang, W. Huang, P. Chen, *ACS Nano* **2012**, *6*, 3206-3213; c) S. Głab, A. Hulanicki, G. Edwall, F. Ingman, *Crit. Rev. Anal. Chem.* **1989**, *21*, 29-47; d) D. Zappa, V. Galstyan, N. Kaur, H. M. M. Munasinghe Arachchige, O. Sisman, E. Comini, *Anal. Chim. Acta* **2018**, *1039*, 1-23; e) N. B rsan, U. Weimar, *J. Phys. Condens. Matt.* **2003**, *15*, R813-R839.

[11] a) B. Hasenknopf, R. Delmont, P. Herson, P. Gouzerh, *Eur. J. Inorg. Chem.* **2002**, 1081-1087; b) P. F. Wu, P. C. Yin, J. Zhang, J. Hao, Z. C. Xiao, Y. G. Wei, *Chem.-Eur. J.* **2011**, *17*, 12002-12005; c) A. Blazevic, A. Rompel, *Coord. Chem. Rev.* **2016**, *307*, Part 1, 42-64; d) H. Ai, Y. Wang, B. Li, L. Wu, *Eur. J. Inorg. Chem.* **2014**, 2766-2772.

[12] A. Guinier, G. Fournet, C. B. Walker, F. D. Carlson, Small-Angle Scattering of X-Rays, JOHN WILEY, **1955**.

[13] T. Kojima, M. R. Antonio, T. Ozeki, *J. Am. Chem. Soc.* **2011**, *133*, 7248-7251.

[14] M. M. Pierce, C. S. Raman, B. T. Nall, *Methods* **1999**, *19*, 213-221.

[15] S. J. Pike, J. J. Hutchinson, C. A. Hunter, *J. Am. Chem. Soc.* **2017**, *139*, 6700-6706.

[16] a) H. Yu, Z. Wu, Z. Wei, Y. Zhai, S. Ru, Q. Zhao, J. Wang, S. Han, Y. Wei, *Commun. Chem.* **2019**, *2*, 15; b) H. Yu, Y. Zhai, G. Dai, S. Ru, S. Han, Y. Wei, *Chem. Eur. J.* **2017**, *23*, 13883-13887; c) H. Yu, S. Ru, G. Dai, Y. Zhai, H. Lin, S. Han, Y. Wei, *Angew. Chem. Int. Ed.* **2017**, *56*, 3867-3871.

[17] C. Martin, C. Lamonier, M. Fournier, O. Mentré, V. Harlé, D. Guillaume, E. Payen, *Inorg. Chem.* **2004**, *43*, 4636-4644.